05

Initiation of the accumulation of microcracks in granite under combined static and impact loading. Trigger effect

© I.P. Shcherbakov, Kh.F. Makhmudov, A.E. Chmel

Ioffe Institute,
194021 St. Petersburg, Russia
e-mail: chmel@mail.ioffe.ru

Received April 12, 2023
Revised September 13, 2023
Accepted October 8, 2023

The hypocenter accumulation and crack propagation processes were studied in a laboratory model experiment. The impact wave in the uniaxially compressed granite was excited by a pendulum directed transversely to the compression. The acoustic emission method was used for recording the release of energy during the accumulation of microcracks and the formation of local damage. It was found that release of energy of microcracks induced by the pendulum under static pressure far from the pre-measured threshold of the sample global failure has several stages with a different slope of the accumulation curve. The impact damage threshold decreased by 5−20% in case of an increase of the compressive pressure on the sample depending on the installed pendulum energy, i.e. a trigger effect was manifested.

Keywords: granite, impact fracture, acoustic emission, trigger effect.

DOI: 10.61011/JTF.2024.01.56900.86-23

Introduction

The interest in the phenomenon of trigger failure i.e. the loss of equilibrium of a large-scale infrastructure system in a metastable state (destruction of an underground structure, rock caving, failure of the offshore coastal structures) under a minor external impact of natural (background seismic activity [1], volcanic activity [2], tides [3], atmospheric phenomena [4]) and anthropogenic origin [5–7] emerged already in the last century, when the impact of the construction of large-scale water reservoirs on the seismic activity of the regions was registered.

Laboratory studies and modeling of trigger situations are conducted in addition to field observations [8–11]. The experiments related to unresolved problems affecting the probability of trigger failures, such as the initial degree of the rock damage [12,13] or the presence of residual deformations [14] are of particular interest.

Subthreshold „rock„ failure is often observed under the laboratory conditions using the acoustic emission (AE) method, which is sensitive to elastic waves emitted when microcracks emerge in loaded solids. Various load application geometries are used for such observations, in particular, triaxial [15,16] or uniaxial [17] compression, as well as shear [18,19] and impact [20] loads. The AE method was also used to detect microcracks in granites caused by high-temperature heating [21] or rapid cooling [22].

Many publications noted the close simulation of field situations by laboratory load application patterns for AE monitoring of the failure development [23,24]. In this study, the static vertical loading of the sample was combined with a point impact in the horizontal direction which simulates the predominant vertical mechanical stress in rocks in the field conditions with the orthogonal action of other force factors listed above [1–3,5–7].

Granite samples that were uniaxially loaded from stable to pretrigger states were used for studying the fracture propagation. The accumulation of mechanical microdefects in the material exposed to single impact wave is considered in this paper. The AE method was used to measure the energy released by the formation of microcracks with nanosecond time resolution. Special attention was paid to the initial stage of the energy release pattern under various combinations of static and dynamic loading.

1. Samples and equipment

Westerly granite blocks with a size of $32 \times 20 \times 10$ mm were used as samples. The acoustic studies of the behavior of Westerly granite under mechanical load were started in the last century [17,25] and actively continued until the last decade [22,26,27]. The density of this material is 2650 g/cm^3; the typical grain and pore sizes are 0.8 and 0.6 mm, respectively [13].

A laboratory hydraulic press was used for testing. The test setup (Fig. 1) applied mutually perpendicular loads: vertical uniaxial loading with a press and horizontal impact by a pointed striker with a pendulum rod. The sample was placed under the ram of the press in front of the thrust plate, which prevented its horizontal displacement under the striker impact at low pressures.

The granite destruction threshold (main fracturing or total crushing) was preliminarily determined under uniaxial compression at pressure of Q_{th} without impact. The reproducibility of the destructive pressure in various samples

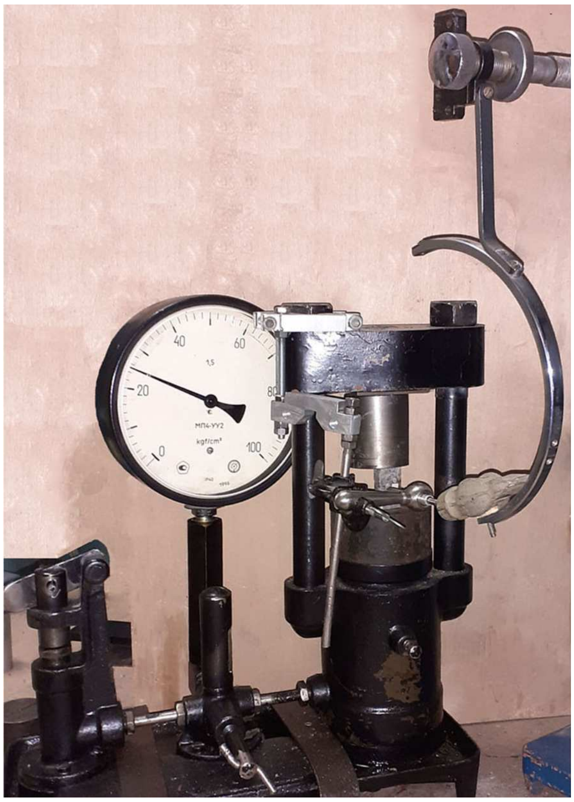

Figure 1. Image of the test setup for recording of AE caused by the impact failure.

(10 measurements were made, 1 sample returned inconsistent result) was ±2% of the average value.

The striker impact caused local damage to the sample surface. The energy of impact of the striker on the sample E was set at 0.06, 0.12 and 0.18 J by changing the pendulum height.

For AE recording, a broadband piezoelectric sensor made of highly sensitive $Pb(Zr_xTi_{1-x})O_3$ ceramics was attached with mastic to the impacted surface of the sample. AE signals were recorded in the computer memory with a time resolution of 40 ns using analog-to-digital converter ASK-3106. AE pulses with a frequency of up to 500 kHz were processed by digital low-pass filtering at the level of 80 kHz for elimination of the effect of vibrations of the test setup components.

Acoustic response was measured at 1) press pressure $Q = 0$; 2) pressure $Q = 0.5Q_{th}$; 3) minimum pressure $Q < Q_{th}$, at which the sample was destroyed with a given impact energy (trigger effect). Each combination of static pressure Q and energy E was repeated 3–5 times until a reproducible result was obtained, i.e. generation of acoustic emission scans with similar intensity and duration.

2. Results and discussion

The AE signal was recorded during 2 ms after the striker touched the surface of the sample. The amplitude squared of the acoustic pulse, A^2, is proportional to the energy E released as a result of the microcrack formation. The increasing sum of pulse energies with the AE generation reflected the accumulation of microcracks that formed after the striker impact. The accumulation curves plotted related to the three above-mentioned impact energies are shown in Fig. 2–4. Each figure shows the development of damage in the samples at zero pressure (Fig. 2, a–4, a) and two compressive pressures of the press equal to 0.5 of the destructive pressure in static mode (Fig. 2, b–4, b) and

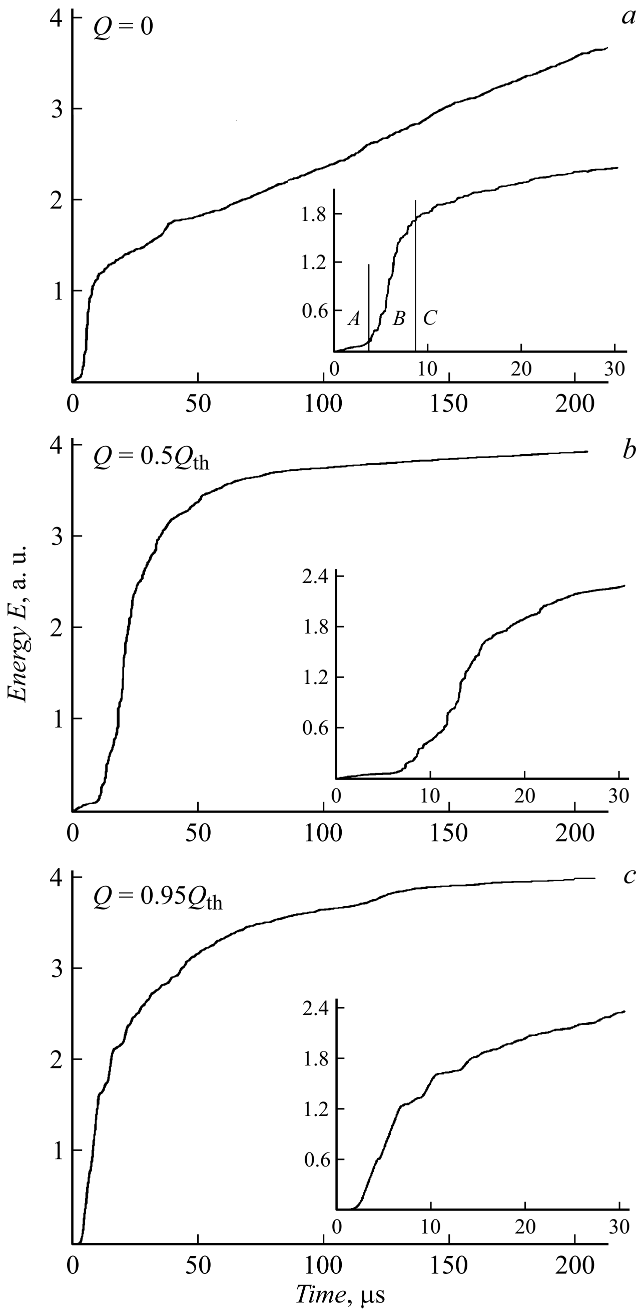

Figure 2. Here and in Fig. 3, 4 — curves of acoustic energy released after the impact damage of samples; the insets show the initial sections of the curves on an enlarged scale. Striker impact energy 0.06 J.

some pressure $Q < Q_{\mathrm{th}}$, resulting in fatal destruction of the sample by the strike (Fig. 2, c–4, c).

One can see that the accumulation curves consist of three elements that manifest themselves in combinations or as stand-alone curves. The accumulation of microcracks in the initial section of the curves initiated by impacts with an energy of 0.06 (Fig. 2) and 0.12 J (Fig. 3) at pressures $Q = 0$ and $Q = 0.5Q_{\mathrm{th}}$ is slow, with a very slight slope of the curves. „Decelerated" sections (designated as zone A in Fig. 2) have a duration of $5-10\,\mu$s and are replaced by accelerated accumulation of defects —slope of the curves increases sharply. The duration of the fragment of „rapid" growth — $10-15\,\mu$s (zone B). It is followed by a smooth subsiding growth of the curves of the energy released by microcracks (zone C).

Based on the structure of a strong but heterogeneous mineral, the following interpretation of the three stages of local damage development can be proposed. The „deceleration" of the initial section of microcrack growth is explained by some plasticity of the porous material with minimum discontinuity. The reservoir of conditionally „weak points" in the sample volume is quickly depleted after reaching the

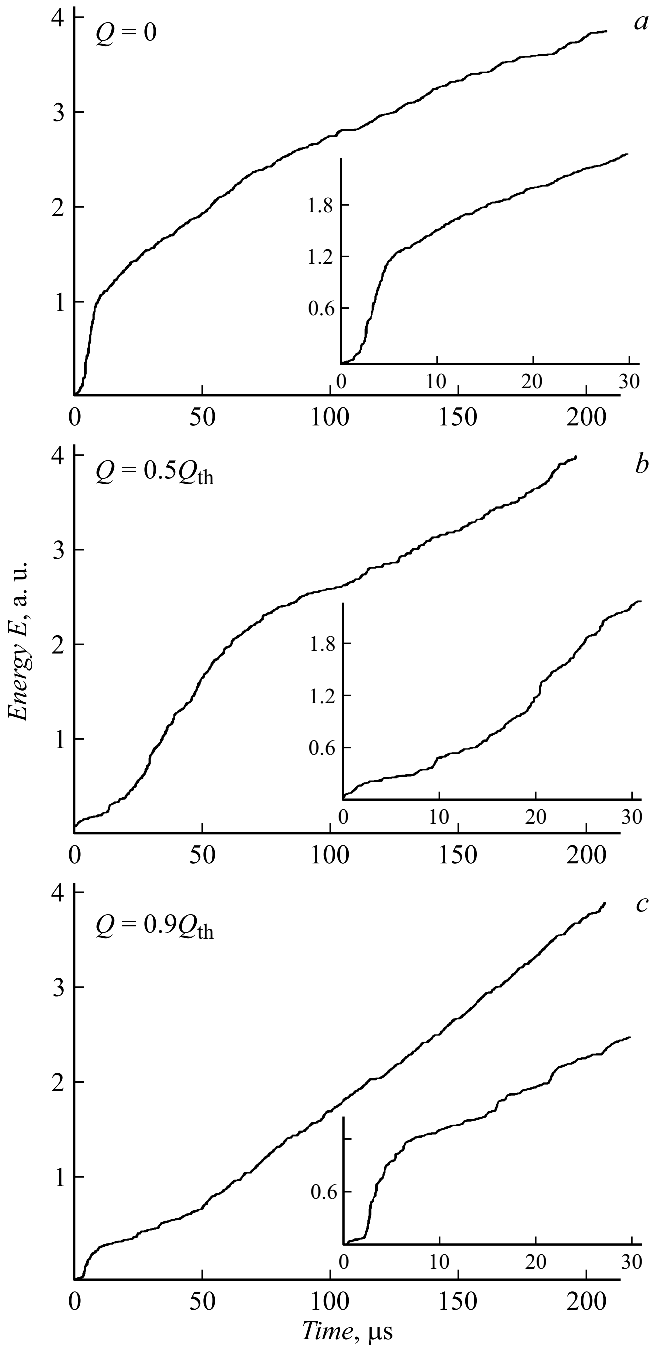

Figure 3. Similar to Fig. 2. Impact energy 0.12 J.

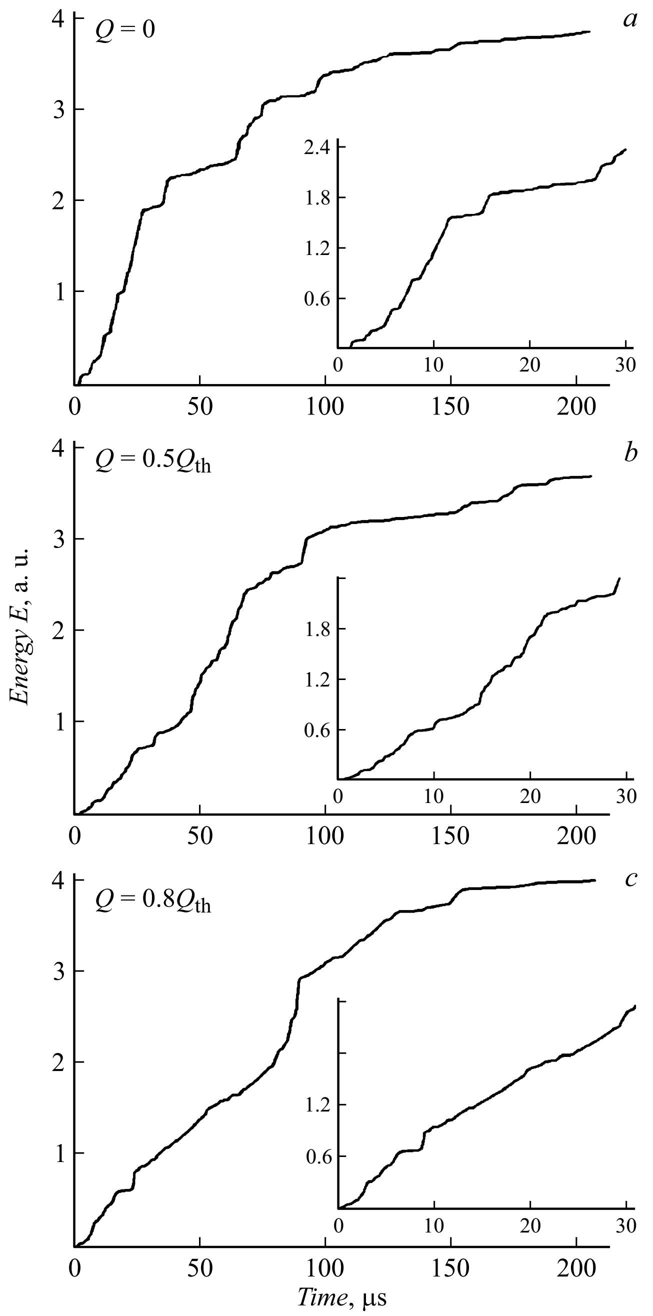

Figure 4. Similar to Fig. 2. Impact energy 0.18 J.

yield stress in 5–10 μs during the following 10–15 μs and smoother accumulation of microcracks commences from more stable areas.

It's worth noting that the slope of the curves on a prolonged final section is lower at an impact energy of 0.006 J (Fig. 2, *a, b*) than at an energy of 0.012 J (Fig. 3, *a, b*). Consequently, the accumulation of microcracks was faster under the exposure to higher energy.

The impact of the striker caused damage to the surface with a linear size of 0.5–1 mm at zero static pressure. Trigger failures occurred in the sample with the formation of main cracks (outside the sweep duration of 2 ms) when the sample was compressed to a pressure of $Q = 0.95Q_{\text{th}}$ upon impact with an energy of 0.006 J, as well as to a pressure of $Q = 0.9Q_{\text{th}}$ upon impact with an energy of 0.012 J.

The character of the curves did not vary in the initial section at the maximum impact energy (0.18 J). In addition, the broken curves indicates less orderly energy emissions instead of a monotonous, smooth process of material degradation. A strong trigger effect occurred at a pressure of $Q = 0.8Q_{\text{th}}$ macroscopic destruction of the sample with disintegration into small fragments.

Conclusion

The comparison of the energy accumulation curves for the formation of microcracks in case of local impact damage of granite at compressive pressures of $Q = 0$ and $0.5Q_{\text{th}}$ showed that three stages can be defined in the energy output mode under these conditions:

a) brief (under these experimental conditions 5–10 μs) insignificant energy release during plastic deformation of the material with minimal destruction of the structure;

b) intensive destruction process due to the destruction of existing „weak points" (10–15 μs);

c) the attenuating process of accumulation of microcracks with the formation of point the surface damage with a linear size of ~ 1 mm.

A trigger effect occurred as the compression of the samples increased: the threshold of catastrophic destruction dropped by 5% at an impact energy of 0.06 J; by 10% at 0.12 J and by 20% at 0.18 J. The above-mentioned transients were not observed in the latter case. „Asymptomatic" initiation of damage development indicates a high degree of danger of the behavior of objects located in the zone of impact of the above-mentioned factors contributing to „pre-threshold" destruction.

Conflict of interest

The authors declare that they have no conflict of interest.

References

[1] Y. Jin, N. Dyaur, Y. Zheng. Seismic Record., **1**, 66 (2021). DOI: 10.1785/0320210015
[2] J.C. Lahr, B.A. Chouet, C.D. Stephens, J.A. Power, R.A. Page. J. Volcanol. Geotherm. Res., **309**, 139 (1994). DOI: 10.1016/0377-0273(94)90031-0
[3] C.H. Scholz, Y.J. Tan, F. Albino. Nature Commun., **10**, Article N 2526 (2019). DOI: 10.1038/s41467-019-10605-2
[4] W. Fan, J.J. McGuire, C.D. de Groot-Hedlin, M.A.H. Hedlin, S. Coats, J.W. Fiedler. Geophys. Res. Lett., **46**, 12909 (2019). DOI: 10.1038/s41467-019-10605-2
[5] V.V. Adushkin. Geologiya i geofizika, **5**, (709), (2018) (in Russian). DOI: 10.15372/GiG20180510
[6] A.F. Emanov, A.A. Emanov, A.V. Fateev, E.V. Shevkunova, V.G. Podkorytova, O.V. Kuprish. Ross. sejsmologicheskij zhurn., **2**, 88 (2020) (in Russian). DOI: 10.35540/2686-7907.2020.3.08
[7] T. Chelidze, T. Matcharashvili, V. Mepharidze, N. Dovgal. Entropy, **25**, 467 (2023). DOI: 10.3390/e25030467
[8] A.P. Bobryakov. FTPRPI, **6**, 35 (2013) (in Russian).
[9] I.P. Shcherbakov, H.F. Makhmudov, A.E. Chmel. FTPRPI, **6**, 64 (2022) (in Russian).
[10] V.A. Novikov, V.I. Okunev, V.N. Klyuchkin. *Triggernye effekty v geosistemakh.* Materialy IV Vseross. konf. s mezhdunarodnym uchastiem (6–9 June, M., 2017), p. 171 (in Russian).
[11] V.A. Novikov, V.I. Okunev, V.N. Klyuchkin, J. Liu, Yu.Ya. Ruzhin, X. Shen. Earthq. Sci., **30**, 167 (2017). DOI: 10.1007/s11589-017-0181-8
[12] J. Jiang, G. Su, X. Zhang, X.-T. Feng. Bull. Eng. Geol. Environ., **79**, 3175 (2020). DOI: 10.1007/s10064-020-01760-8
[13] L.Q. Chen, J.S. Zhang, J.H. Chen, J.G. Chen. J. Cent. South Univ., **48**, 484 (2017). DOI: 10.11817/j.issn.1672-7207.2017.02.028
[14] H. Xu, X.-T. Feng, Ch. Yang, X. Zhang, Y. Zhou, Zh. Wang. Int. J. Rock Mech. Min. Sci., **117**, 90 (2019). DOI: 10.1016/j.ijrmms.2019.03.013
[15] B. Haimson, C. Chang. Int. J. Rock. Mech. Min., **37**, 285 (2000). DOI: 10.1016/S1365-1609(99)00106-9
[16] S. Stanchits. *Proceedings of the First Southern Hemisphere International Rock Mechanics Symposium, Australian Centre for Geomechanics* (2008), p. 69. DOI: 10.36487/ACG_repo/808_154
[17] C.H. Sondergeld, L.H. Estey. JGR Solid Earth, **86**, 2915 (1981). DOI: 10.1029/JB086iB04p02915
[18] X. Lei. Appl. Sci. **9**, 2498 (2019). DOI: 10.3390/app9122498
[19] P.A. Johnson, J. Carmeliet, H.M. Savage, M. Scuderi, B.M. Carpenter, R.A. Guyer, E.G. Daub, C. Marone. Geophys. Res. Lett., **43**, 1559 (2016). DOI: 10.1002/2015GL067056
[20] X. Liu, M. Pan, X. Li, J. Wang. *Proceedings of the World Conference on Acoustic Emission–2015* (Springer Proceedings in Physics, 179), p. 135.
[21] L. Griffiths, O. Lengliné, M.J. Heap, P. Baud, J. Schmittbuhl. JGR Solid Earth., **123**, 2246 (2018). DOI: 10.1002/2017JB015191
[22] X. Jinyong, Ch. Zhanqing, W. Jiangyu. J. Eng. Geol., **29**, 508 (2021). DOI: 10.13544/j.cnki.jeg.2019-473
[23] X. Lei, S. Ma. Earthquake Sci., **27**, 627 (2014). DOI: 10.1007/s11589-014-0103-y
[24] G.C. McLaskey, D.A. Lockner. Int. J. Rock. Mech., **110**, 97 (2018). DOI: 10.1016/j.ijrmms.2018.07.001

[25] P. Tapponnier, W.F. Brace. Int. J. Rock Mech. Mining Sci. Geomech. Abstr., **13**, 1976, 103 (1976). DOI: 10.1016/0148-9062(76)91937-9
[26] P. Kolář, M. Petružálek, T. Lokajíček, J. Šílený, Z. Jechumtálová, P. Adamová, A. Boušková. Pure Appl. Geophys., **177**, 4271 (2020). DOI: 10.1007/s00024-020-02517-w
[27] A. Blanke, G. Kwiatek, T.H.W. Goebel, M. Bohnhoff, G. Dresen. Geophys. J. Int., **524**, 1371 (2020). DOI: 10.1093/gji/ggaa524

Translated by A.Akhtyamov